THE JOURNAL OF BIOLOGICAL CHEMISTRY VOL. 283, NO. 19, pp. 13437–13449, May 9, 2008
Printed in the U.S.A.

TLR4 Signaling Is Coupled to SRC Family Kinase Activation, Tyrosine Phosphorylation of Zonula Adherens Proteins, and Opening of the Paracellular Pathway in Human Lung Microvascular Endothelia*

Received for publication, September 24, 2007, and in revised form, February 6, 2008 Published, JBC Papers in Press, March 7, 2008, DOI 10.1074/jbc.M707986200

Ping Gong[‡§1], Daniel J. Angelini[‡§], Shiqi Yang[‡¶], Guanjun Xia[‖], Alan S. Cross[**], Dean Mann[§], Douglas D. Bannerman[‡‡], Stefanie N. Vogel[§§], and Simeon E. Goldblum[‡§¶2]

*From the [‡]Mucosal Biology Research Center, [§]Department of Pathology, [¶]Department of Medicine, [§§]Department of Microbiology and Immunology, [‖]Department of Pharmaceutical Sciences, and **Center for Vaccine Development, University of Maryland, Baltimore, Maryland 21201 and the [‡‡]Bovine Functional Genomics Laboratory, United States Department of Agriculture, Beltsville, Maryland 20705*

Bacterial lipopolysaccharide (LPS) is a key mediator in the vascular leak syndromes associated with Gram-negative bacterial infections. LPS opens the paracellular pathway in pulmonary vascular endothelia through protein tyrosine phosphorylation. We now have identified the protein-tyrosine kinases (PTKs) and their substrates required for LPS-induced protein tyrosine phosphorylation and opening of the paracellular pathway in human lung microvascular endothelial cells (HMVEC-Ls). LPS disrupted barrier integrity in a dose- and time-dependent manner, and prior broad spectrum PTK inhibition was protective. LPS increased tyrosine phosphorylation of zonula adherens proteins, VE-cadherin, γ-catenin, and p120^{ctn}. Two SRC family PTK (SFK)-selective inhibitors, PP2 and SU6656, blocked LPS-induced increments in tyrosine phosphorylation of VE-cadherin and p120^{ctn} and paracellular permeability. In HMVEC-Ls, c-SRC, YES, FYN, and LYN were expressed at both mRNA and protein levels. Selective small interfering RNA-induced knockdown of c-SRC, FYN, or YES diminished LPS-induced SRC Tyr^{416} phosphorylation, tyrosine phosphorylation of VE-cadherin and p120^{ctn}, and barrier disruption, whereas knockdown of LYN did not. For VE-cadherin phosphorylation, knockdown of either c-SRC or FYN provided total protection, whereas YES knockdown was only partially protective. For p120^{ctn} phosphorylation, knockdown of FYN, c-SRC, or YES each provided comparable but partial protection. Toll-like receptor 4 (TLR4) was expressed both on the surface and intracellular compartment of HMVEC-Ls. Prior knockdown of TLR4 blocked both LPS-induced SFK activation and barrier disruption. These data indicate that LPS recognition by TLR4 activates the SFKs, c-SRC, FYN, and YES, which, in turn, contribute to tyrosine phosphorylation of zonula adherens proteins to open the endothelial paracellular pathway.

Gram-negative sepsis is a persistent and widespread problem, with up to 300,000 cases occurring each year in the United States alone (1). Despite the development of new antibiotics, mortality from Gram-negative sepsis remains unacceptably high (2). Life-threatening Gram-negative sepsis can be complicated by systemic vascular collapse, disseminated intravascular coagulation, and vascular leak syndromes, including the acute respiratory distress syndrome (3, 4). One common element to these sepsis-associated vascular complications is the presence of endothelial cell (EC)[3] injury and/or dysfunction. Evidence exists that the bacterial component responsible for much of these EC alterations is the bacterial outer membrane constituent, endotoxin or lipopolysaccharide (LPS). LPS bioactivity has been detected in the bloodstream of Gram-negative septicemic patients, and levels of circulating LPS predict development of multiorgan failure, including acute respiratory distress syndrome (5). Administration of LPS alone to experimental animals reconstitutes the EC injury associated with sepsis (3, 4). Finally, immunological and pharmacological interventions that specifically target the LPS molecule, at least in some reports, protect against these same vascular complications (6, 7). Although LPS stimulates release of endogenous mediators that are known to increase endothelial paracellular permeability (8–10), LPS also directly opens the paracellular pathway (11).

TLR4 (Toll-like receptor 4) is the principal signal-transducing receptor for LPS (12). C3H/HeJ mice with a missense mutation (P712H) in TLR4 and C57BL/10ScCr mice with a deletion mutation in TLR4 both are unresponsive to LPS (12, 13). The signaling elements downstream to TLR4 have been thoroughly studied in cells of monocyte/macrophage lineage that express TLR4 and CD14 on the cell surface (12). Although it is well known that LPS elicits a wide range of host cell responses, reports on downstream TLR4 signaling have almost exclusively focused on proinflammatory gene expression. Whether these

* This work was supported, in whole or in part, by National Institutes of Health Grants HL-70155 and HL-84223 (to S. E. G.) and AI-18797 (to S. N. V.). The costs of publication of this article were defrayed in part by the payment of page charges. This article must therefore be hereby marked "*advertisement*" in accordance with 18 U.S.C. Section 1734 solely to indicate this fact.

[1] Recipient of American Heart Association (Mid-Atlantic Affiliate) Postdoctoral Fellowship 0725389U.

[2] To whom correspondence should be addressed: Mucosal Biology Research Center, University of Maryland School of Medicine, 20 Penn St., HSF II-Rm. 351, Baltimore, MD 21201. Tel.: 410-706-5504; Fax: 410-706-5508; E-mail: sgoldblu@mbrc.umaryland.edu.

[3] The abbreviations used are: EC, endothelial cell; LPS, lipopolysaccharide; PTK, protein-tyrosine kinase; SFK, SRC family PTK; TNF-α, tumor necrosis factor α; ZA, zonula adherens; BSA, bovine serum albumin; HMVEC-L, human lung microvascular endothelial cell; RT, reverse transcription; PVDF, polyvinylidene difluoride; FITC, fluorescein isothiocyanate; ELISA, enzyme-linked immunosorbent assay; VEGF, vascular endothelial growth factor; siRNA, small interfering RNA; IL, interleukin.

findings can be extended either to other cell types, including ECs, and/or to other biological activities, including tyrosine phosphorylation events and barrier disruption, is less clear.

In ECs, LPS responsiveness is less well understood. First, there is no agreement as to whether EC TLR4 is expressed within the cell or on the cell surface (14–17). In immortalized human dermal microvascular ECs (HMEC-1), immunostaining of TLR4 was evident on the cell surface (16), and anti-TLR4 antibodies blocked LPS-induced NF-κB activation (17). In other reports, however, TLR4 was not detectable on either HMEC-1 cells (18) or human umbilical vein ECs (19) by surface staining using these same anti-TLR4 antibodies. In the latter report, anti-TLR4 antibodies, at concentrations that far exceeded those that blocked LPS responsiveness in macrophages, failed to block the human umbilical vein EC response to LPS (14). In another report in which flow cytometry was applied to human coronary artery ECs, five distinct anti-TLR4 antibodies failed to detect surface TLR4, and these same antibodies could not block LPS-induced EC expression of CD62E (E-selectin) (15). There is precedent for TLR4 as an intracellular receptor in respiratory and intestinal epithelia (20, 21). These combined studies raise the possibility that TLR4 is predominantly or exclusively expressed intracellularly in ECs. In multiple studies, ECs did not express CD14 (22, 23). In one recent report, early passage human umbilical vein ECs were found to synthesize and express low levels of CD14 on the cell surface (2000–3000 molecules/cell) that rapidly diminished with subsequent passage (24). In another report, anti-CD14 antibodies, in the absence of serum, reduced the EC response to LPS (25). These inconsistent findings for TLR4 and CD14 expression in ECs have made the molecular mechanisms for LPS responsiveness in these cells more difficult to define.

In a bovine EC system, we have found that LPS increases tyrosine phosphorylation of EC proteins enriched to EC-EC boundaries, reorganizes the actin cytoskeleton, and opens the paracellular pathway, all in a PTK-dependent manner (11, 26). The operative PTK(s) and their EC-EC junctional substrates were unknown. LPS has been shown to activate multiple PTKs, including Bruton's tyrosine kinase (27, 28), SRC family PTKs (SFKs) (29, 30), proline-rich tyrosine kinase 2 (31), Syk (32), and Ron receptor tyrosine kinase (33). LPS increases tyrosine phosphorylation of multiple host proteins, including several components of specialized intercellular junctions, such as connexin 43 and PECAM-1 (34, 35). Several established mediators of vascular permeability, such as histamine (36), TSP-1 (37), SPARC (38), VEGF (39), and tumor necrosis factor α (TNF-α) (10), each increase tyrosine phosphorylation of one or more proteins within the EC-EC adherens junction, the zonula adherens (ZA). The ZA is a multiprotein complex that couples the subcortical actin cytoskeleton to the cytoplasmic domain of cadherins, surface receptors that mediate homophilic cell-cell adhesion (40, 41). Changes in the tyrosine phosphorylation state of one or more ZA proteins alter protein-protein interactions within the multiprotein complex that promote actin depolymerization, ZA disassembly, and/or disruption of the ZA-actin cytoskeletal linkage (10, 36, 39). Through inside-out signaling, homophilic adhesion between opposing VE-cadherin ectodomains is thus reduced, and the endothelial paracellular pathway opens.

In this study, we have identified specific LPS-inducible PTK(s) that participate in increased tyrosine phosphorylation of EC substrates, including ZA proteins, leading to opening of the paracellular pathway in human lung microvascular endothelia.

MATERIALS AND METHODS

Reagents—Protein-free *Escherichia coli* K235 LPS (<0.008% protein) was prepared by modification of the phenol/water extraction method to exclude contaminating bacterial constituents present in commercial LPS preparations (42). The broad spectrum PTK inhibitors, herbimycin A and geldanamycin, and the SFK inhibitors, PP2 and Su6656, were purchased from Calbiochem. LPS derived from *E. coli* O111:B4 and [^{14}C]bovine serum albumin (BSA) were purchased from Sigma.

EC Culture—Human lung microvascular ECs (HMVEC-Ls) and, in selective experiments, human pulmonary artery ECs (Cambrex, San Diego, CA) were cultured in EC growth medium (EBM-2; Cambrex) containing 5% fetal bovine serum, human recombinant epidermal growth factor, human recombinant insulin-like growth factor-1, human basic fibroblast growth factor, vascular endothelial growth factor, hydrocortisone, ascorbic acid, gentamicin, and amphotericin B (10). Only ECs at passages 5–10 were studied. Trypan blue exclusion was used to assess EC plasma membrane integrity or viability.

Assay of Transendothelial Albumin Flux—Transendothelial BSA flux was assayed as previously described (6). Briefly, gelatin-impregnated polycarbonate filters (13-mm diameter, 0.4-μm pore size) (Nucleopore, Pleasanton, CA) mounted in polystyrene chemotactic chambers (ADAPS, Dedham, MA) were inserted into wells of 24-well plates. ECs (2×10^5 cells/chamber) were seeded in each upper compartment and cultured for 72 h. The base-line barrier function of each monolayer was established by introducing an equivalent concentration of the permeability tracer, [^{14}C]BSA (1.1 pmol (*i.e.* 4800–6200 dpm/0.5 ml)) to each upper compartment for 1 h, after which 0.5 ml from the lower compartment was mixed with 4.5 ml of Optifluor scintillation fluid (Packard Instruments, Downers Grove, IL) and counted in a liquid scintillation counter (Beckman, Fullerton, CA). Only those monolayers retaining ≥97% of the tracer were utilized in experiments. The monolayers were then exposed to increasing concentrations of protein-free LPS, Pam3Cys (L2000; EMC Microcollections, Tuebingen, Germany), or medium alone for increasing exposure times in the presence or absence of PTK inhibitors, after which transendothelial [^{14}C]BSA flux was again assayed.

Expression of SFKs and TLR4 in HMVEC-Ls—Total RNA was isolated from HMVEC-Ls with the Absolutely RNA Miniprep kit (Stratagene, La Jolla, CA). A human SRC family kinase MultiGene-12^{TM} RT-PCR profiling kit (SuperArray, Frederick, MD) was used to detect mRNA for the eight human SFK members. Primers used to detect *TLR4* mRNA by RT-PCR were 5′-CGGATGGCAACATTTAGAATTAGT-3′ (forward) and 5′-TGATTGAGACTGTAATCAAGAACC-3′ (reverse). To assess expression at the protein level, total HMVEC-L lysates were resolved by 4–12% gradient SDS-PAGE (Invitrogen) and transferred onto polyvinyldene difluoride (PVDF) membranes (Millipore, Bedford, MA). The blots were probed with murine

monoclonal antibodies raised against c-SRC, LYN (Upstate Biotechnology, Inc., Lake Placid, NY), and YES (BD Biosciences), rabbit polyclonal anti-FYN antibodies, or murine monoclonal antibodies raised against TLR4 (Santa Cruz Biotechnology, Inc., Santa Cruz, CA). Blots were washed and incubated with horseradish peroxidase-conjugated rabbit anti-mouse antibody or goat anti-rabbit antibody (BD Biosciences) and developed with ECL (Amersham Biosciences). In other experiments, HMVEC-Ls were detached using 0.25% trypsin-EDTA, in some cases permeabilized with 0.1% Triton X-100, incubated with fluorescein isothiocyanate (FITC)-conjugated mouse anti-human TLR4 antibodies (BD Biosciences) or a FITC-conjugated species- and isotype-matched control antibody for 30 min at 4 °C in phosphate-buffered saline. Antibody binding to the intact and permeabilized cells was evaluated using a flow cytometer (FACSCAN; BD Biosciences), and the data were analyzed with CELLQUEST software (BD Biosciences).

Phosphotyrosine Immunolocalization—Postconfluent ECs were exposed for 1 h to LPS (100 ng/ml) or medium alone. The ECs were fixed (4% paraformaldehyde, 10 min), washed, permeabilized (0.1% Triton X-100, 5 min), blocked, and incubated for 1.5 h with FITC-conjugated anti-phosphotyrosine antibodies (4G10; Millipore) in the dark. The ECs were mounted on microscope slides, visualized, and photographed through a fluorescence microscope (Nikon Eclipse TE 2000-E).

Phosphotyrosine Immunoblotting—Postconfluent ECs (2.3×10^5 cells/100-mm dish) were exposed to LPS or medium alone, after which they were lysed with ice-cold modified radioimmunoprecipitation assay buffer, containing 50 mM Tris-HCl, pH 7.4, 1% Nonidet P-40, 0.25% sodium deoxycholate, 150 mM NaCl, 1 mM EGTA, 100 mg/ml type-1 DNase, 1 mM sodium orthovanadate, 1 mM NaF, 1 mg/ml pepstatin A, 10 mM pyrophosphate, and 1 mM phenylarsine oxide (all purchased from Sigma), and 1 tablet of complete protease inhibitor mixture (Roche Applied Science) per 20 ml of lysate as described (10). The lysates were centrifuged, and the supernatants were assayed for protein concentration with a Bradford protein assay kit (Bio-Rad). The samples were resolved by 4–12% gradient SDS-PAGE and transferred onto PVDF membranes. The blots were blocked with membrane blocking solution (Zymed Laboratories Inc., San Francisco, CA) and were incubated with mouse anti-phosphotyrosine antibodies (PY-Plus mixture) (Zymed Laboratories Inc.), followed by horseradish peroxidase-conjugated rabbit anti-mouse antibody (BD Biosciences), and developed with ECL. To confirm equivalent protein loading and transfer, blots were stripped with the Blot Restore membrane rejuvenation kit (Chemicon, Temecula, CA), reprobed with mouse anti-β-tubulin antibodies (Zymed Laboratories Inc.), and again developed with ECL as described (10).

Identification of Phosphotyrosine-containing Proteins—An immunoprecipitation strategy was employed to identify ZA substrates for LPS-induced tyrosine phosphorylation as described (43). Lysates of ECs treated with LPS or medium alone were precleared by incubation with either anti-murine or anti-rabbit IgG cross-linked to agarose (Sigma) for 1 h at 4 °C and then incubated overnight at 4 °C with specific murine monoclonal antibodies raised against β-, γ-, or p120-catenin (BD Biosciences) or a rabbit polyclonal antibody raised against VE-cadherin (Cayman, Ann Arbor, MI). The resultant immune complexes were immobilized by incubation with IgG cross-linked to agarose for 2 h at 4 °C, centrifuged, washed, boiled for 7 min in sample buffer, and again centrifuged. The supernatants were then processed for phosphotyrosine immunoblotting with PY-Plus mixture as described above. To control for immunoprecipitation efficiency and protein loading and transfer, blots were stripped and reprobed with the immunoprecipitating antibody. Immunoblots were captured for quantitative densitometry using a FUJIFILM LAS-3000 imaging system (FUJIFILM, Greenwood, SC), and each phosphotyrosine signal was normalized to its respective total signal on the same blot.

Detection of SFK Activity by Cell-based ELISA—HMVEC-Ls (1.5×10^4 cells/well) were cultured for 48 h in flat bottom 96-well plates, after which they were exposed for increasing times to increasing concentrations of LPS. The cells were fixed, washed, quenched with H_2O_2 and NaN_3, and microwaved, according to the manufacturer's protocol (SuperArray). The plates were washed, blocked, incubated with anti-phospho-SRC (Tyr^{416}) or anti-pan-SRC antibodies, washed, and incubated with secondary antibody. The plates were incubated with developing solution, and the $A_{450\ nm}$ for each well was determined. To normalize each well to relative cell number, the plates were washed, dried, incubated with protein stain, again washed, and solubilized in 1% SDS, and the $A_{595\ nm}$ was determined. Each phospho-SRC and each pan-SRC well was normalized to cell number in the same well, and each normalized phospho-SRC value was normalized to its normalized pan-SRC value. SFK activity was calculated as phospho-SRC A_{450}/A_{595} per pan-SRC A_{450}/A_{595}.

Knockdown of TLR4 and SFKs through Small Interfering RNA (siRNA)—SMARTPool siRNA duplex products designed to target *TLR4*, c-*SRC*, *FYN*, *LYN*, and *YES*, as well as control siRNA duplexes (Dharmacon, Lafayette, CO), were preincubated with TransMessenger transfection reagent (Qiagen, Valencia, CA), and the complexes were presented to HMVEC-Ls for 3 h in the absence of serum. At 72 h, ECs were lysed and processed for immunoblotting with anti-c-SRC, anti-FYN, anti-LYN, or anti-YES antibodies. TLR4 immunoblotting was performed at 24 h. To confirm equivalent protein loading and transfer, blots were stripped and reprobed with anti-β-tubulin antibody and developed with ECL. Once knockdown was established, the siRNAs were transfected into ECs for studies of SFK activation, ZA protein tyrosine phosphorylation, and transendothelial [^{14}C]BSA flux. For the barrier assays, HMVEC-Ls were cultured to 70% confluence in plastic dishes, after which they were transfected with siRNA targeting *FYN*, c-*SRC*, *LYN*, *YES*, *TLR4*, or control siRNAs. After 24 h, the transfected cells were seeded into assay chambers and cultured for 48 h, after which the baseline barrier function was established. Only EC monolayers that retained ≥97% of the tracer molecule were exposed for 6 h to 100 ng/ml LPS or medium alone and again assayed for transendothelial [^{14}C]BSA flux.

Statistics—One-way analysis of variance with repeated measures, followed by *post hoc* comparisons using Tukey's multiple paired comparison test, was used to compare the mean responses among experimental and control groups for all

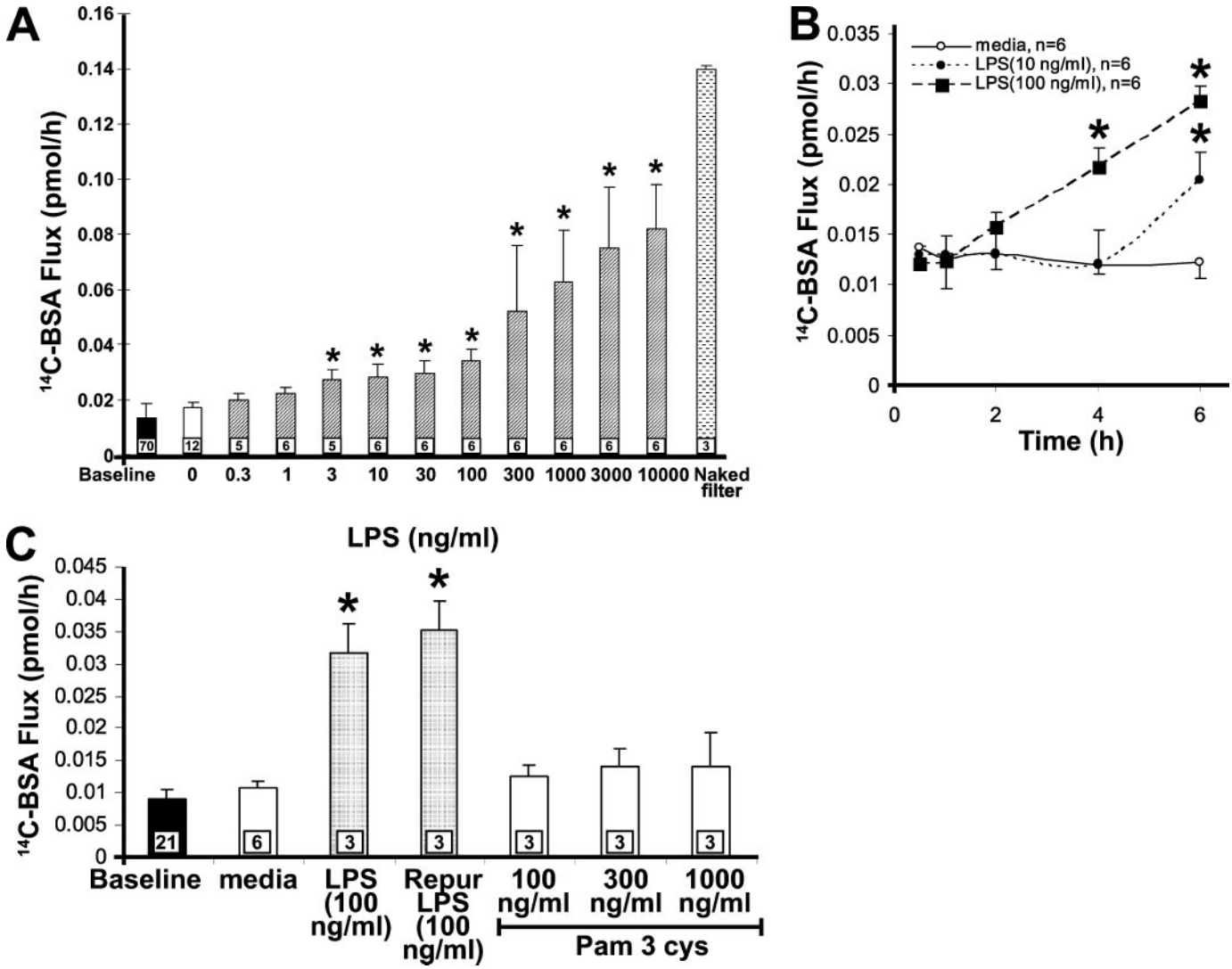

FIGURE 1. **LPS increases paracellular permeability across HMVEC-Ls.** Postconfluent HMVEC-L monolayers were exposed for 6 h to increasing concentrations of LPS (*A*) or to one of two fixed concentrations of LPS (10 or 100 ng/ml) or medium alone for increasing exposure times (*B*). *C*, in other studies, postconfluent HMVEC-L monolayers were exposed for 6 h to equivalent concentrations of LPS *versus* protein-free LPS that lacks contaminating TLR2 agonists, increasing concentrations of Pam3cys, an established TLR2 agonist, or medium alone. *Vertical bars* represent mean ± S.E. transendothelial [^{14}C]BSA flux in pmol/h immediately after the study period. Mean ± S.E. pretreatment base-line transendothelial [^{14}C]BSA flux is indicated by the *closed bars* in *A* and *C*, and flux across naked filters is shown by the *stippled bar* in *A*. *n* indicates number of monolayers studied and in *A* and *C* is indicated *within* each *bar*. In *B*, the *n* for each time point within each group was 6. *, significantly increased compared with the simultaneous medium control at $p < 0.05$; **, significantly decreased compared with LPS alone at $p < 0.05$. The data in *A* and *B* each were the cumulative result of three independent experiments with 2–6 replicates/treatment/experiment, whereas the data in *C* were obtained from two experiments with three replicates/treatment/experiment.

experiments. The GraphPad PRISM 4 program for windows was used for these analyses. A p value of <0.05 was considered significant.

RESULTS

LPS Increases Transendothelial [^{14}C]BSA Flux across HMVEC-Ls—Although we have demonstrated that LPS increases the paracellular permeability through PTK activation in bovine ECs, there are well known species differences in LPS responsiveness (44). Accordingly, we studied the effect of LPS on barrier function in human ECs. At 6 h, LPS induced a dose-dependent increase in [^{14}C]BSA flux across HMVEC-L monolayers (Fig. 1*A*). The minimum LPS concentration that increased albumin flux compared with the medium control was 3 ng/ml. The maximal increase in albumin flux, 0.082 pmol/h, was seen with 10,000 ng/ml of LPS. The LPS effect was also time-dependent (Fig. 1*B*). HMVEC-L monolayers were exposed to either of two fixed concentrations of LPS (10 and 100 ng/ml) or medium alone for increasing exposure times (0.5–6 h). Exposure to either 10 or 100 ng/ml LPS was associated with prolonged stimulus-to-response lag times of 4 and 6 h, respectively. Finally, a highly purified LPS preparation that lacks contaminating lipoproteins that activate TLR2 (42) induced the same EC response as unpurified LPS (Fig. 1*C*). At the same time, a known TLR2 agonist, the triacylated lipopeptide, Pam3Cys, did not increase transendothelial [^{14}C]BSA flux at concentrations that activate TLR2 in monocytes (45). Terminal dUTP nick-end labeling assays excluded HMVEC-L apoptosis after LPS treatment (300 ng/ml, 6 h), and a trypan blue exclusion assay indicated that barrier dysfunction in response

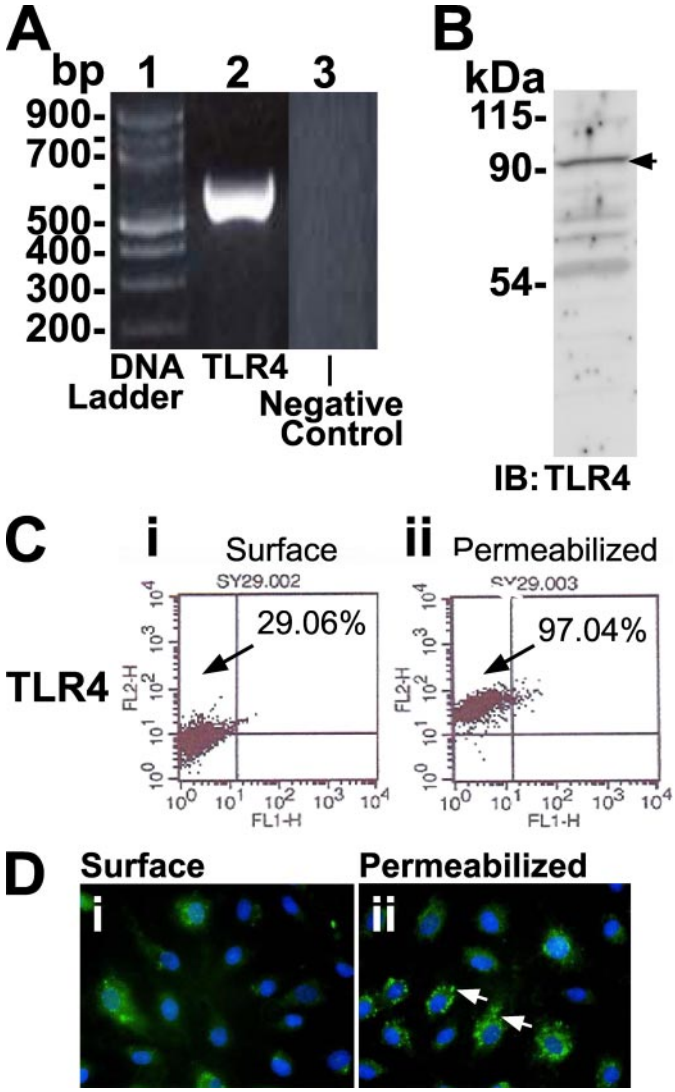

FIGURE 2. **TLR4 Expression in HMVEC-Ls.** *A*, RNA was isolated from HMVEC-Ls and cDNA generated using oligo(dT) primers and reverse transcriptase. This cDNA was used as a template for amplification with DNA polymerase and primers corresponding to *TLR4* (*lane 2*). Base pairs (*bp*) and control DNA ladder are indicated on the *left* (*lane 1*). PCR mixture without DNA template as a negative control is indicated in *lane 3*. These RT-PCR experiments were performed twice. *B*, HMVEC-L lysates were resolved by SDS-PAGE and transferred to PVDF, and blots were probed for TLR4. Molecular masses in kDa are indicated on the *left*. *IB*, immunoblot. This blot is representative of three experiments. *C*, nonpermeabilized (*i*) and permeabilized (*ii*) HMVEC-Ls were studied by flow cytometry for TLR4. This study is representative of three experiments. *D*, postconfluent HMVEC-Ls were fixed and, in selected experiments, were permeabilized, blocked, and incubated with anti-TLR4 antibodies followed by fluoroprobe-labeled secondary antibodies. Nuclei were counterstained with 4′,6-diamidino-2-phenylindole. *i*, surface TLR4; *ii*, total cell TLR4. *Green*, TLR4; *blue*, nuclei. The *arrows* indicate perinuclear TLR4 staining. Magnification was ×400. These photomicrographs are representative of two experiments.

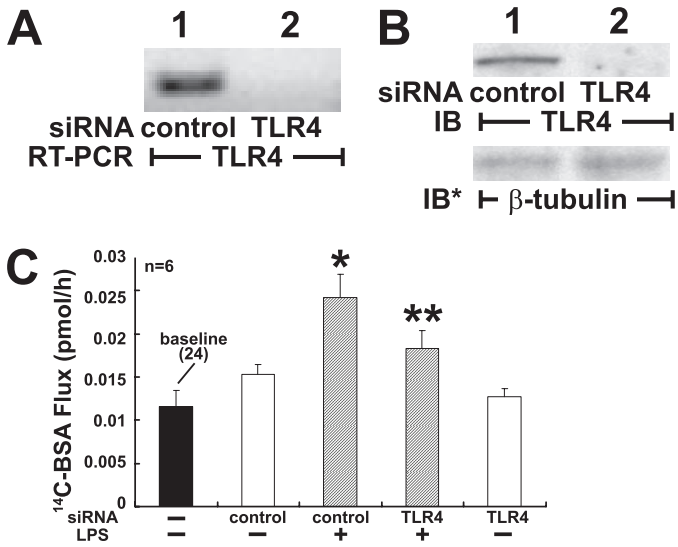

FIGURE 3. **Role of TLR4 in LPS-induced barrier disruption.** HMVEC-Ls were transfected with TLR4-targeting or control siRNAs for 24 h. *A*, RT-PCR was applied to detect mRNAs for TLR4. *B*, HMVEC-Ls were processed for immunoblotting for TLR4, and each blot was stripped and reprobed for β-tubulin. *IB*, immunoblot; *IB**, immunoblot after stripping. These blots are representative of ≥3 experiments. *C*, for the barrier assay, HMVEC-Ls cultured to 70% confluence in plastic dishes were transfected with siRNA targeting TLR4 or control siRNAs. Transfected cells were seeded onto the filters in assay chambers and cultured for 24 h, after which base-line barrier function was established. Only EC monolayers that retained ≥97% of the tracer molecule were exposed for 6 h to 100 ng/ml LPS or medium alone and again assayed for transendothelial [^{14}C]BSA flux. *Vertical bars* represent mean ± S.E. transendothelial [^{14}C]BSA flux in pmol/h immediately after the 6-h study period. *n*, the numbers of wells studied, was 6 for each group, and these data were the cumulative result of three independent experiments with two replicates/treatment/experiment. *, significantly increased compared with the control siRNA group at $p < 0.05$; **, significantly decreased compared with LPS and control siRNA at $p < 0.05$.

to LPS could not be ascribed to loss of EC viability (data not shown). Therefore, the LPS-induced increase in transendothelial [^{14}C]BSA flux was dose- and time-dependent and could not be ascribed to lipoprotein contamination, loss of plasma membrane integrity, or EC apoptosis.

TLR4 Expression in HMVEC-Ls—We utilized RT-PCR and immunoblotting to establish whether TLR4 mRNA and/or protein were expressed in HMVEC-Ls (Fig. 2, *A* and *B*). TLR4 was clearly expressed in HMVEC-Ls at both the mRNA and protein levels. Nonpermeabilized and permeabilized HMVEC-Ls were studied by flow cytometry for TLR4 expression in three independent experiments (Fig. 2*C*). TLR4 was expressed in 98.8, 97.0, and 99.4% of permeabilized cells (Fig. 2*C*, *ii*), whereas surface expression of TLR4 was detected only on 29.1, 29.0, and 16.4% of cells (Fig. 2*C*, *i*). Fluorescence microscopy of nonpermeabilized (surface staining) and permeabilized (total cell staining) HMVEC-Ls (Fig. 2*D*) confirmed that TLR4 was predominantly expressed intracellularly and was immunolocalized to the perinuclear area (Fig. 2*D*, *ii*).

Requirement for TLR4 in LPS-induced Barrier Disruption—HMVEC-Ls were transfected with TLR4-targeting or control siRNAs, and after 24 h, the HMVEC-Ls were processed for RT-PCR and immunoblotting for TLR4 (Fig. 3, *A* and *B*). Both TLR4 mRNA (Fig. 3*A*) and protein (Fig. 3*B*) were knocked down >95%. In the barrier assay, prior TLR4 knockdown protected against >65% of the LPS-induced increase in transendothelial [^{14}C]BSA flux. These combined data indicate that, in HMVEC-Ls, TLR4 is required for LPS-induced barrier disruption.

LPS Increases Transendothelial [^{14}C]BSA Flux through PTK Activation—We had shown previously that LPS-induced barrier disruption is PTK-dependent (11), but which PTK was operative was not determined. Preincubation for 2 h with either of two structurally and functionally dissimilar, broad spectrum PTK inhibitors, herbimycin A (1.0 μM) or geldanamycin (0.5 μM), reduced the LPS-induced increase in albumin flux by

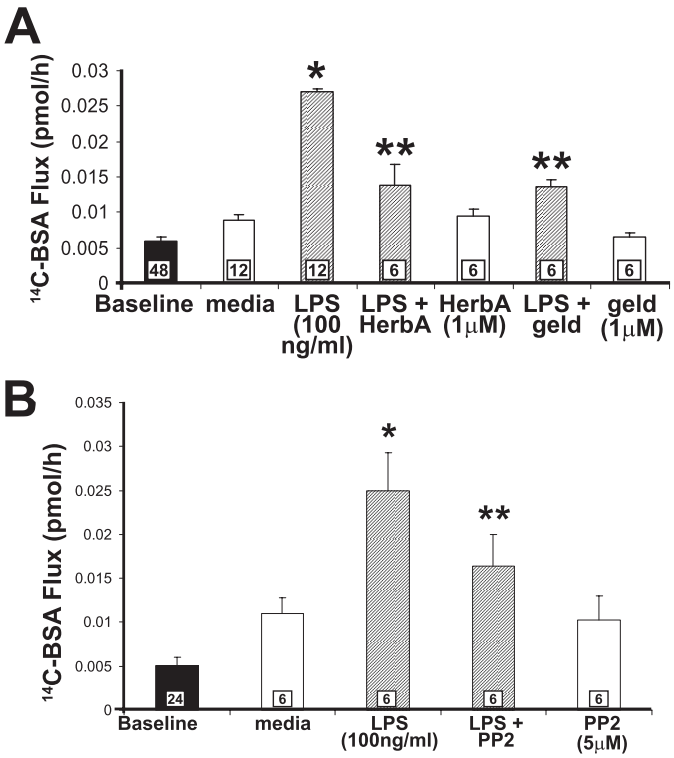

FIGURE 4. **Role of PTKs in LPS-induced barrier disruption.** *A*, LPS (100 ng/ml) was presented to HMVEC-L monolayers in the presence and absence of either of two broad spectrum PTK inhibitors, herbimycin A (*HerbA*) (1 μM) or geldanamycin (*geld*) (1 μM), or monolayers were treated with each agent or medium alone. *B*, postconfluent HMVEC-Ls cultured in barrier assay chambers were exposed for 6 h to LPS (100 ng/ml) or medium alone in the presence or absence of PP2 (5 μM). *Vertical bars* represent mean ± S.E. transendothelial [^{14}C]BSA flux in pmol/h immediately after the 6-h study period. Mean ± S.E. pretreatment base-line transendothelial [^{14}C]BSA flux is indicated by the *closed bars*. *n* indicates the number of monolayers studied and is indicated *within* each *bar*. Data were generated from ≥3 independent experiments with 2–3 replicates/treatment/experiment. *, significantly increased compared with the medium control at $p < 0.05$; **, significantly decreased compared with LPS alone at $p < 0.05$.

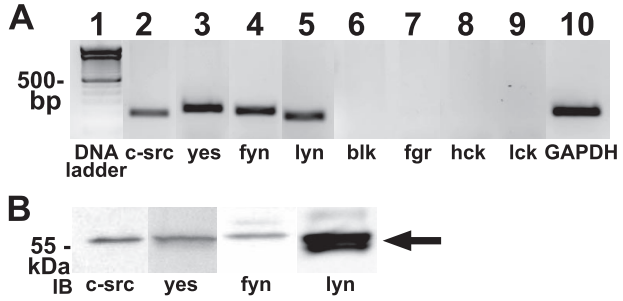

FIGURE 5. **SFK expression in HMVEC-Ls.** *A*, RT-PCR was used to detect mRNAs for the eight human SFKs, c-*SRC*, *YES*, *FYN*, *LYN*, *BLK*, *FGR*, *HCK*, and *LCK*, as well as GAPDH (*lane 10*) as a housekeeping control. Base pairs (*bp*) with control DNA ladder are shown on the *left* (*lane 1*). *B*, HMVEC-L lysates were resolved by SDS-PAGE and transferred to PVDF, and blots were probed with antibodies raised against the four SFKs, expressed in HMVEC-Ls at the mRNA levels, c-SRC, YES, FYN, and LYN. Molecular mass in kDa is indicated on the *left*. The *arrow* on the *right* indicates SFKs. Each of these two blots is representative of two experiments.

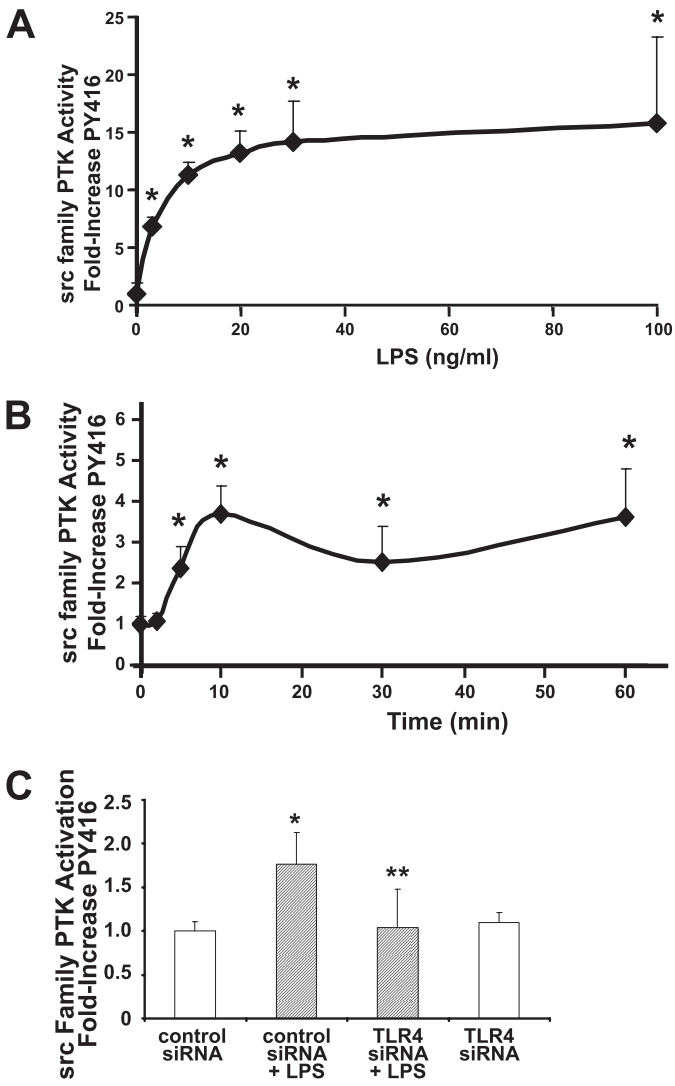

FIGURE 6. **LPS Activates SFK(s) through TLR4.** Postconfluent HMVEC-Ls were exposed to increasing concentrations of LPS or medium alone for increasing exposure times and processed for a cell-based ELISA that detects phosphorylation of Tyr^{416}, the activation site conserved across SFKs. The assay normalizes phospho-Tyr^{416} to total SFK and total cellular protein. SFK activation is expressed as mean ± S.E. -fold increase relative to the simultaneous medium control. *A*, ECs exposed for 10 min to increasing concentrations of LPS ($n = 6$). *B*, ECs exposed for increasing times to LPS (100 ng/ml) or medium alone ($n = 6$). *, significantly increased compared with the simultaneous medium control at $p < 0.01$. *C*, HMVEC-Ls were transfected with TLR4-targeting, or control siRNAs for 24 h and processed for the same ELISA that detects Tyr^{416} phosphorylation. $n = 9$ for each control and experimental group. *, significantly increased compared with the control siRNA group at $p < 0.05$; **, significantly decreased compared with LPS and control siRNA at $p < 0.05$. The data in *A*, *B*, and *C* each were generated from ≥3 independent experiments with 2–3 replicates/treatment/experiment.

>75% (Fig. 4*A*). Each inhibitor alone had no effect on transendothelial albumin flux. To identify which PTK(s) mediates this LPS-induced barrier disruption, we used selective pharmacological PTK inhibitors, including the epidermal growth factor receptor-selective inhibitor, AG1478, the ErbB2-selective inhibitor, AG825, the VEGF receptor-selective inhibitor, Delphian 002, the PDGFR-selective inhibitor, Delphian 005, the Bruton's tyrosine kinase-selective inhibitor, LFM-A13, and SFK-selective inhibitor, PP2. Only pretreatment with PP2 was protective, decreasing the LPS-induced increment in transendothelial [^{14}C]BSA flux by ~60% (Fig. 4*B*) (data not shown).

SFK Expression in HMVEC-Ls—Eight SFKs are expressed in human tissues; some are ubiquitously expressed (*e.g.* c-SRC, FYN, and YES), whereas the expression of others is more restricted (46, 47). In one report, the three ubiquitously

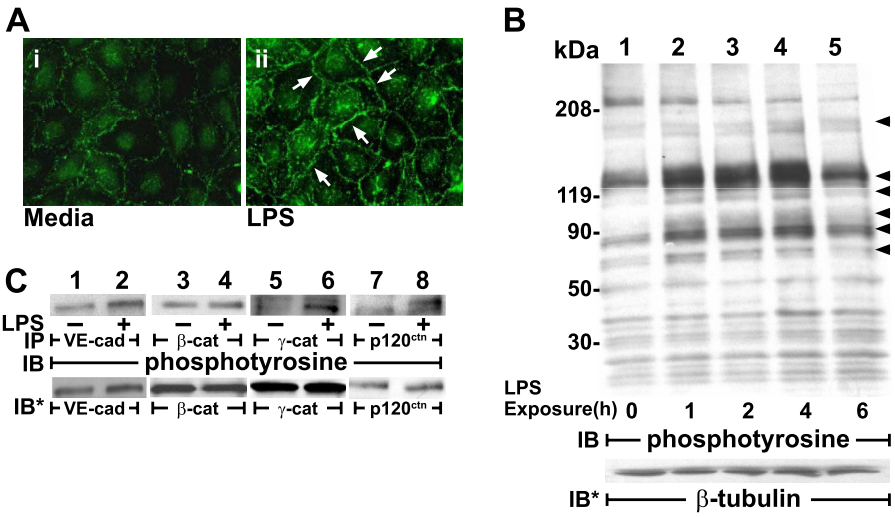

FIGURE 7. **Identification of ZA proteins as substrates for LPS-induced tyrosine phosphorylation.** Postconfluent HMVEC-L monolayers were exposed for varying times to LPS (100 ng/ml) or medium alone. *A*, HMVEC-Ls were fixed, incubated with FITC-conjugated antiphosphotyrosine antibody, and analyzed by fluorescence microscopy. *i*, medium control (1 h); *ii*, LPS (1 h). The *arrows* indicate phosphotyrosine signal at intercellular boundaries. Magnification was ×400. These photomicrographs are representative of two experiments. *B*, in other studies, HMVEC-Ls were exposed to LPS (100 ng/ml) or medium alone in the presence of vanadate (200 μM) and phenylarsine oxide (1.0 μM), only during the last 0.25 h of incubation. HMVEC-L lysates were resolved by SDS-PAGE and transferred to PVDF membranes, and the blots were probed with antiphosphotyrosine antibody. To confirm equivalent protein loading and transfer, blots were stripped and reprobed for β-tubulin. Molecular masses in kDa are indicated on the *left*. The *arrows* on the *right* indicate bands with altered phosphotyrosine signal in response to LPS. This blot is representative of three experiments. *C*, lysates of LPS-treated and medium control HMVEC-Ls were immunoprecipitated with antibodies raised against VE-cadherin (*lanes 1* and *2*), β-catenin (*lanes 3* and *4*), γ-catenin (*lanes 5* and *6*), and p120^{ctn} (*lanes 7* and *8*). The immunoprecipitates were resolved by SDS-PAGE and transferred onto PVDF, and the blots were probed with antiphosphotyrosine antibody. For normalization of phosphotyrosine signal to the immunoprecipitated protein, blots were stripped and reprobed with each immunoprecipitating antibody. Each blot is representative of ≥3 experiments. *IP*, immunoprecipitate; *IB*, immunoblot; *IB**, immunoblot after stripping.

expressed SFKs, c-SRC, YES, and FYN, were detected in human dermal microvascular endothelial cells (48). In another study, LYN was detected within ECs that comprise the murine blood brain barrier (49). In HMVEC-Ls, we sought to measure mRNA expression of the eight human SFKs. We detected mRNA for c-*SRC*, *YES*, *FYN*, and *LYN* but not *BLK*, *FGR*, *HCK*, or *LCK* (Fig. 5*A*). We then used specific antibodies raised against the four SFKs detected in HMVEC-Ls at the mRNA level, c-SRC, YES, FYN, and LYN, to probe for their protein products (Fig. 5*B*). All four proteins were detected at their anticipated gel mobilities. These combined data indicate that c-SRC, YES, FYN, and LYN are expressed in HMVEC-Ls at both mRNA and protein levels. To our knowledge, this is the first report of LYN expression in human ECs.

LPS Activates SFKs—To determine whether LPS can activate one or more SFKs in HMVEC-Ls, cells were exposed to increasing concentrations of LPS or medium alone for increasing exposure times. The cells were then processed for a cell-based ELISA that detects phosphorylation of Tyr^{416} (SuperArray), the activation site conserved across SFKs. LPS increased SFK activity in a dose- and time-dependent manner (Fig. 6, *A* and *B*). LPS at concentrations of ≥1 ng/ml increased SFK activity (Fig. 6*A*). At LPS concentrations of ≥30 ng/ml, activation plateaued. A fixed LPS concentration of 100 ng/ml provoked sustained activation from 5 to 60 min (Fig. 6*B*), temporally proximal to LPS-induced opening of the paracellular pathway (Fig. 1*B*). Prior knockdown of TLR4 with siRNA in HMVEC-Ls markedly reduced LPS-induced SFK activation (Fig. 6*C*). These data indicate that LPS-induced SFK activation can be coupled to TLR4.

Identification of Substrates for LPS-induced Tyrosine Phosphorylation—As a first step to identify those EC proteins that might be tyrosine-phosphorylated in response to LPS, postconfluent HMVEC-L monolayers were exposed to LPS (100 ng/ml) or medium alone and probed with FITC-conjugated anti-phosphotyrosine antibody for fluorescence microscopy, as described (11). LPS-exposed ECs displayed enhanced fluorescence signal predominately restricted to intercellular boundaries (Fig. 7*A*, *ii*) compared with the medium control (Fig. 7*A*, *i*). These data suggest that LPS preferentially stimulates tyrosine phosphorylation of proteins that are either enriched to or, upon phosphorylation, translocate to cell-cell junctions in postconfluent endothelia. To characterize further these substrates for LPS-induced tyrosine phosphorylation, total lysates of HMVEC-Ls exposed to LPS (100 ng/ml) for increasing exposure times (1–6 h) or medium alone were processed for phosphotyrosine immunoblotting. To optimize the phosphotyrosine signal, the protein-tyrosine phosphatase inhibitors, sodium orthovanadate (200 μM) and phenylarsine oxide (1 μM), were added 15 min prior to EC lysis. LPS increased tyrosine phosphorylation of multiple EC proteins (Fig. 7*B*). More specifically, bands that migrated with gel mobilities indicative of molecular masses of ~185, 140–120, 105, 88, and 66 kDa displayed increased phosphotyrosine signal compared with the medium control. Several phosphotyrosine-containing bands displayed distinct phosphorylation kinetics. The tyrosine phosphorylation states of phosphoproteins with molecular masses between 88 and 180 kDa peaked at 4 h, whereas the 66-kDa protein peaked at 1 h. The 220-kDa protein was dephosphorylated over time. On the basis of subcellular localization (Fig. 7*A*) and gel mobility (Fig. 7*B*), we adopted an immunoprecipitation/immunoscreening strategy to determine whether ZA proteins might be substrates for LPS-induced tyrosine phosphorylation. LPS increased tyrosine phosphorylation of the ZA proteins (Fig. 7*C*), VE-cadherin (*lanes 1* and *2*), γ-catenin (*lanes 5* and *6*), and p120 catenin (*lanes 7* and *8*) compared with the simultaneous medium control. Upon quantitative densitometry, tyrosine phosphorylation of VE-cadherin ($n = 3$), γ-catenin ($n = 3$), and p120^{ctn} ($n = 3$), was increased 1.8 ± 0.1-, 2.1 ± 0.3-, and 2.3 ± 0.7-fold, respectively, in response to LPS (Fig. 7*C*) (data not shown). In contrast, no change in β-catenin tyrosine phosphorylation was detected (*lanes 3* and *4*). Therefore, in HMVEC-Ls,

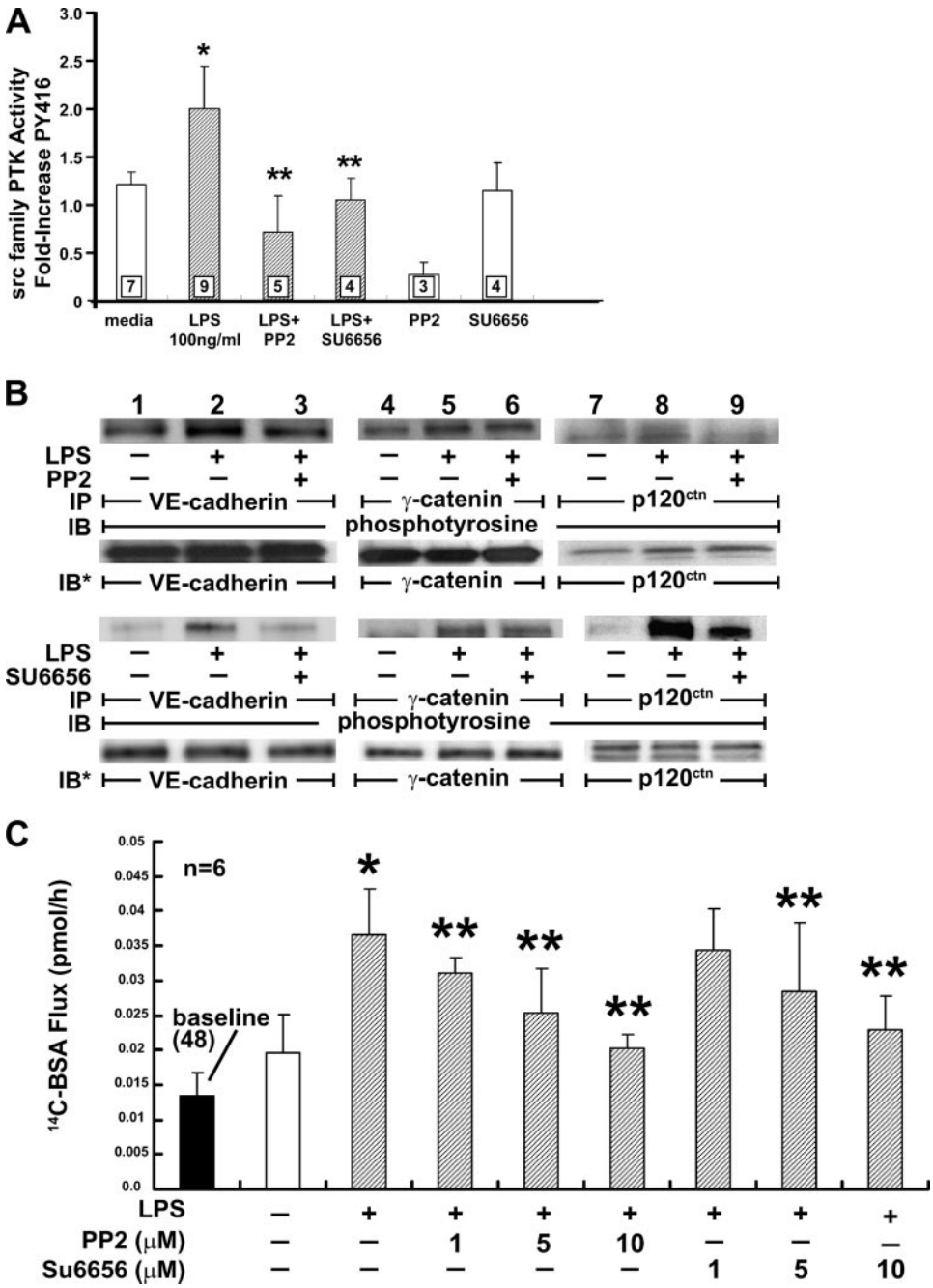

FIGURE 8. **LPS increases tyrosine phosphorylation of ZA proteins and endothelial paracellular permeability through SFK(s) activation.** *A*, ECs exposed to LPS (100 ng/ml) or medium alone in the presence or absence of either of two SFK-selective inhibitors, PP2 or SU6656 (10 μM), were processed for a cell-based ELISA that detects Tyr^{416} phosphorylation. SFK activation is expressed as mean ± S.E. -fold increase relative to the simultaneous medium control. *n*, the number of monolayers studied, is indicated *within* each *bar*. *B*, HMVEC-Ls were exposed for 4 h to LPS (100 ng/ml) or medium alone in the presence or absence of PP2 (5 μM) or SU6656 (10 μM) as well as in the presence of vanadate (200 μM) and phenylarsine oxide (1.0 μM), only during the last 0.25 h of incubation. ECs were lysed and immunoprecipitated with antibodies against VE-cadherin (*lanes 1–3*), γ-catenin (*lanes 4–6*), and $p120^{ctn}$ (*lanes 7–9*). The immunoprecipitates were resolved by SDS-PAGE and transferred to PVDF, and the blots were probed with antiphosphotyrosine antibody. Blots were stripped and reprobed with the respective immunoprecipitating antibodies. *IP*, immunoprecipitate; *IB*, immunoblot; *IB**, immunoblot after stripping. These blots are representative of ≥3 experiments. *C*, postconfluent human pulmonary artery ECs cultured in barrier assay chambers were exposed for 6 h to LPS (100 ng/ml) or medium alone in the presence or absence of increasing concentrations of PP2 or SU6656. *Vertical bars* represent mean ± S.E. transendothelial [^{14}C]BSA flux in pmol/h immediately after the 6-h study period. The mean ± S.E. pretreatment base lines are indicated in *C* by the *closed bar*. In *C*, the number of monolayers studied was six for each condition. *, significantly increased compared with the simultaneous medium control at $p < 0.05$; **, significantly decreased compared with LPS alone at $p < 0.05$. The data in *A* and *C* each were generated from three independent experiments with 2–3 replicates/treatment/experiment.

ZA proteins are selectively tyrosine-phosphorylated by SFKs in response to LPS.

Participation of SFKs in the EC Response to LPS—Since LPS activates SFKs (Fig. 6, *A* and *B*) and increases tyrosine phosphorylation of ZA proteins (Fig. 7*C*), and SFK-selective PTK inhibition protects against LPS-induced loss of barrier function (Fig. 4*B*), we asked whether SFK catalytic activity might be involved in ZA protein phosphorylation and/or opening of the paracellular pathway. The SFK-selective inhibitors, PP2 (10 μM) (50) and SU6656 (10 μM) (51), each profoundly reduced SFK activation in response to LPS (Fig. 8*A*). Both PP2 and SU6656 also diminished LPS-induced increases in tyrosine phosphorylation (Fig. 8*B*) of VE-cadherin (*lane 3*) and p120 catenin (*lane 9*) but failed to block γ-catenin phosphorylation (*lane 6*). Using quantitative densitometry, PP2 protected against LPS-induced VE-cadherin ($n = 5$) and $p120^{ctn}$ ($n = 4$) phosphorylation by ~79 and ~89%, respectively, whereas SU6656 provided ~82% ($n = 3$) and ~67% ($n = 3$) protection, respectively (Fig. 8*B* and Table 1). In human pulmonary artery ECs, PP2 and SU6656 both protected against LPS-induced barrier disruption in a dose-dependent manner (Fig. 8*C*). At 10 μM, each blocked almost 100% of the LPS-induced effect. These studies indicate that one or more SFKs participate in LPS-induced increases in both tyrosine phosphorylation of VE-cadherin and p120 catenin and paracellular permeability.

Knockdown of SFKs through siRNA in HMVEC-Ls and LPS-induced EC Responses—To determine which of the four SFKs expressed in HMVEC-Ls were operative in LPS-induced EC responses, HMVEC-Ls were transfected with siRNAs targeting c-*SRC*, *YES*, *FYN*, or *LYN* or control siRNA, as described (10). After 72 h, each SFK protein was knocked down >95% compared with the simultaneous control without off-target, cross-knockdown of other SFKs (Fig. 9*A*). Prior knock-

TABLE 1
SFK-selective inhibition blocks LPS-induced ZA protein tyrosine phosphorylation

ZA protein	LPS	LPS + PP2	*n*	Protection	LPS	LPS + SU6656	*n*	Protection
				%				%
VE-cadherin	1.5 ± 0.1[a]	1.1 ± 0.1	5	78.9[b]	2.2 ± 0.3	1.2 ± 0.1	3	82.1[b]
p120^{ctn}	2.1 ± 0.3	1.1 ± 0.3	4	88.6[b]	5.7 ± 1.2	2.5 ± 0.4	3	66.7[b]

[a] Quantitative densitometry of phosphotyrosine signal for each ZA protein normalized to total ZA protein signal and expressed as -fold increase relative to the simultaneous medium control. *n*, number of independent experiments.
[b] Significant at $p < 0.05$.

down of c-SRC, FYN, or YES significantly reduced LPS-induced SFK Tyr^{416} phosphorylation, whereas knockdown of LYN had no such effect (Fig. 9*B*). Prior knockdown of either c-SRC or FYN each completely blocked LPS-induced tyrosine phosphorylation of VE-cadherin ($p < 0.001$) (Fig. 9, *C* and *D*). Knockdown of YES was only ~70% protective ($p < 0.05$), whereas knockdown of LYN had no effect. In contrast, for p120^{ctn} tyrosine phosphorylation, although prior knockdown of FYN, c-SRC, or YES each was highly (76–84%) protective ($p < 0.001$), none of these treatments provided complete protection against the LPS stimulus (Fig. 9, *C* and *D*). Again, knockdown of LYN had no effect. Taken together, LPS-induced tyrosine phosphorylation of both VE-cadherin and p120^{ctn} was FYN-, c-SRC-, and YES-dependent. However, for VE-cadherin phosphorylation, a hierarchy of SFK participation, in which FYN and c-SRC clearly exceeded YES, was evident. In barrier assays, knockdown of FYN, c-SRC, or YES protected against LPS-induced barrier disruption by 60, 78, and 70%, respectively, whereas, again, LYN knockdown had no such effect (Fig. 9*E*). Therefore, SFKs exhibit both unique functions, as is the case for c-SRC and FYN in VE-cadherin phosphorylation, as well as redundant, overlapping functions, as seen for c-SRC, FYN, and YES in p120^{ctn} tyrosine phosphorylation and barrier disruption.

DISCUSSION

LPS directly increases paracellular permeability across postconfluent HMVEC-L monolayers through TLR4-mediated SFK activation. In our system, LPS at ≥1 ng/ml activated SFKs, and at ≥3 ng/ml, it increased transendothelial albumin flux (Figs. 1 and 3). Circulating LPS levels in sepsis patients reportedly range between 0.26 and 300 ng/ml (52, 53). Since LPS associates with circulating lipoproteins (54), is rapidly cleared by the reticuloendothelial system (55), and nonspecifically inserts itself into lipid membranes, these levels may understate the levels of LPS presented to the host. LPS is continuously shed from the outer membranes of rapidly proliferating bacteria, and this release can be further increased up to ~200-fold through antibiotic-induced bacterial lysis (56, 57). During endotoxemia, the endothelium responds not only to LPS itself but, simultaneously, to numerous endogenous mediators, such as TNF-α, interleukin (IL)-1β, interferons, and others (8–10). Several of these cytokines, such as interferon-γ, IL-2, and IL-1β (58–60), act synergistically with LPS to provoke EC responses. For all of these reasons, the LPS concentrations that were active in our system are pathophysiologically relevant.

In response to various stimuli, endothelial paracellular permeability increases over two distinct time frames: immediate (<30 min) and delayed (2–6 h). Agonists, such as histamine (61), thrombin (62), bradykinin, and platelet-activating factor (63), provoke immediate changes in permeability. However, agonists, such as TNF-α (10), IL-1 (64), thrombospondin-1 (37), and SPARC (38), each elicit a delayed response. The prolonged LPS stimulus-to-response lag times are compatible with this latter category. However, LPS at 100 ng/ml provoked sustained SFK activation from 5 min to 60 min (Fig. 6*B*), temporally proximal to LPS-induced barrier disruption (Fig. 1*B*).

TLR4 expression is required for LPS responsiveness (12, 13). In a chimeric murine model, using TLR$^{+/+}$ and TLR$^{-/-}$ knockout mice, EC expression of TLR4 was essential to LPS-induced pulmonary leukostasis, a prerequisite event for granulocyte-dependent, acute lung injury (65). We now have established that TLR4 is expressed on the surface of <30% of HMVEC-Ls (Fig. 2*C*), and this receptor density and distribution is sufficient for LPS responsiveness. This diminished EC surface expression of TLR4 may explain their decreased and/or delayed LPS responsiveness compared with that seen in monocytes and macrophages.

Although most work on TLR4-dependent cellular responses has focused on NF-κB-mediated gene expression, TLR4 is also coupled to other cell responses, such as paxillin tyrosine phosphorylation (31). Here, we demonstrate that in ECs, TLR4 is required for LPS-induced SFK activation (Fig. 6*C*) and barrier disruption (Fig. 3*C*). Recently, we found that SFK activation participates in tyrosine phosphorylation of TLR4 itself (66). Other TLRs may also utilize SFKs for signaling functions. In fact, c-SRC is recruited to TLR3 in response to a double-stranded RNA stimulus (67). Although the signaling element(s) through which TLR4 is coupled to SFK activation is not yet known, previous reports on IL-1 and TNF-α receptor superfamily signaling support TRAF6 as a candidate. In multiple non-EC systems, signaling through these receptors involves interactions between the proline-rich domain within TRAF6 and the Src homology 3 domain of c-SRC (68–70). In our studies in HMVEC-Ls, siRNA-induced knockdown of TLR4 almost completely blocked LPS-induced SFK activation (Fig. 6*C*) but protected against only ~60% of LPS-induced barrier disruption (Fig. 3*C*). Since the half-life of a given protein can profoundly influence knockdown efficiency, we determined that TLR4 protein was knocked down >95% at 24 h but partially recovered by 48 h (data not shown). It is conceivable that during barrier formation (24–72 h) and the barrier assay itself (>6 h), TLR4 protein expression and function may begin to recover. It is also conceivable that one or more other surface receptors may participate in LPS internalization and/or signaling in ECs.

LPS activates multiple PTKs (27–30, 71). Pretreatment of LPS-challenged rats with genistein decreased extravasation of protein and neutrophils into the bronchoalveolar compartment

(72, 73). Prior PTK inhibition also blocked LPS-induced actin reorganization, intercellular gap formation, and endothelial barrier disruption *in vitro* (11). Here, we show that herbimycin A and geldanamycin each block LPS-induced barrier disruption in human pulmonary microvascular endothelia (Fig. 1*C*). Our findings may explain the findings of the previous *in vivo* studies (72, 73). LPS also activates SFKs in a range of host cells and tissues, including monocytes, macrophages, dentritic cells, glioma cells, and rat tail arteries (30, 74–76). CD14, the TLR4 co-receptor, has been shown to associate with SFKs in response to LPS (30). However, whether ECs express CD14 on their surface is unclear (23, 24). Although we found CD14 expressed in 29% of permeabilized HMVEC-Ls, we failed to detect CD14 on the surface of these same cells (data not shown). Whether CD14 is operative in HMVEC-Ls or not, prior knockdown of TLR4 almost completely blocked SFK activation (Fig. 6*C*). This would indicate that CD14 alone is insufficient to support LPS-induced SFK activation. We now find that in HMVEC-Ls, LPS activates

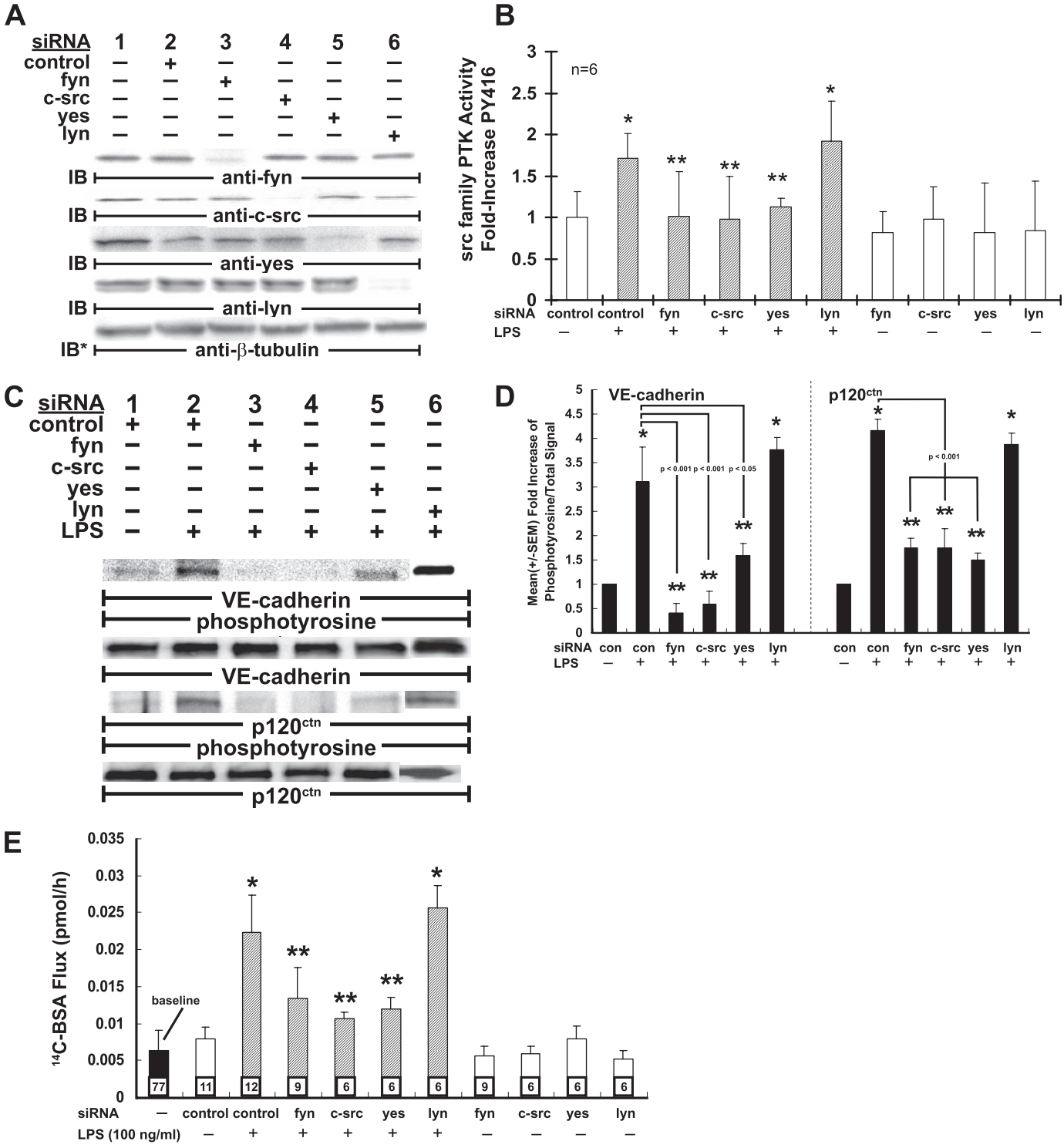

SFKs (Fig. 6, *A* and *B*), c-SRC, FYN, and YES (Fig. 9*B*), in a dose- and time-dependent manner. The kinetics of LPS-induced SFK activation in HMVEC-Ls parallel those described in LPS-treated macrophages (30) and TNFα-treated ECs (10). SFK-selective inhibitors (PP2 and SU6656) attenuate both LPS-induced lung injury and increases in pulmonary vascular permeability *in vivo* (79). Other agonists, such as VEGF and TNFα, also increase endothelial permeability through SFK activation (10, 80). Here, we demonstrate that not only the SFK-selective pharmacological inhibitors, PP2 and SU6656, but also prior knockdown of FYN, c-SRC, and YES, diminish loss of barrier function in response to LPS (Figs. 4*B*, 8*C*, and 9*E*).

LPS, like other established mediators of increased endothelial permeability (10, 36–39), increased tyrosine phosphorylation of one or more proteins enriched to intercellular boundaries (Fig. 7*A*). Specialized EC-EC junctions include the ZA, tight junctions (tj), gap junctions, and PECAM-1. Of interest, SFKs are known to associate with and/or phosphorylate ZA proteins (81), connexins within gap junctions (82, 83), and PECAM-1 (84). Here, we demonstrate that LPS increases tyrosine phosphorylation of VE-cadherin, γ-catenin, and p120 catenin (Fig. 7*C*); prior SFK-selective PTK inhibition prevented phosphorylation of VE-cadherin and p120^{ctn} but not γ-catenin (Fig. 8*B*). c-SRC phosphorylates VE-cadherin at Tyr^{685} in response to VEGF (85), and FYN mediates VE-cadherin tyrosine phosphorylation in response to TNFα (10). Tyrosine phosphorylation of VE-cadherin regulates its binding to catenins and reduces the homophilic adhesion between opposing ectodomains, through inside-out signaling (86). The exact mechanism(s) through which VE-cadherin phosphorylation contributes to LPS-induced opening of the paracellular pathway is unclear. p120^{ctn} was first identified as a substrate for c-SRC (87). It has emerged as a key regulator of cadherin expression and function (86, 88). Whether the ~4-h LPS stimulus-to-barrier response lag time is sufficient to permit changes in VE-cadherin expression that might alter the barrier response to LPS was not addressed here. p120^{ctn} not only regulates VE-cadherin turnover at the plasma membrane but also influences its lateral clustering (86, 88). Phosphorylation of distinct tyrosine or serine/threonine residues within p120^{ctn} determines whether it functions as a positive or negative regulator of cadherin-mediated adhesion (89). This may explain, in part, the inconsistent role of SFKs in cell-cell adhesion (88). β- and γ-catenin compete for the same binding site on the intracellular domain of VE-cadherin. In postconfluent ECs, the formation of mature and cytoskeleton-connected junctions is accompanied by increases in γ-catenin association with VE-cadherin with competitive displacement of β-catenin (90). This might explain why LPS increases tyrosine phosphorylation of γ-catenin but not β-catenin.

SFKs perform both unique and redundant, overlapping functions. LPS activates three SFKs in HMVEC-Ls (Fig. 9*B*). Mice null for each of these SFKs display no phenotypic abnormalities within the lungs or pulmonary vasculature (91). In tissues where multiple SFKs are highly expressed, this has been explained through functional redundancy. After siRNA-mediated specific knockdown of each SFK, three distinct SFKs, FYN, c-SRC, and YES, each participated in tyrosine phosphorylation of VE-cadherin and p120^{ctn} (Fig. 9, *C* and *D*) and the barrier response to LPS (Fig. 9*E*). For p120^{ctn} phosphorylation and barrier disruption, knockdown of any one of these three SFKs failed to result in 100% protection. These results indicate that during the HMVEC-L response to LPS, SFKs clearly perform redundant, overlapping functions. SFKs are also known to perform unique biological functions that cannot be assumed by other family members. c-SRC knock-out mice are resistant to VEGF-induced increases in vascular permeability, whereas FYN knock-out mice are not (77). Prior knockdown of FYN protects against TNFα-induced barrier dysfunction *in vitro*, whereas knockdown of c-SRC or YES do not (10). In the present studies, prior knockdown of either c-SRC or FYN completely blocked tyrosine phosphorylation of VE-cadherin, whereas knockdown of YES was only partially protective (Fig. 9, *C* and *D*). In a recent paper (78), two SFKs, c-SRC and FYN, were found to phosphorylate distinct tyrosine residues within a ZA protein, inducing opposing downstream effects. Whether such differential phosphorylation of VE-cadherin by YES (*versus* either c-SRC or FYN) might explain our findings is unknown. Therefore, in our HMVEC-L system, SFKs perform redundant and possibly unique functions in response to the LPS stimulus.

In summary, LPS increases tyrosine phosphorylation of ZA proteins and paracellular permeability in HMVEC-Ls through

FIGURE 9. **Knockdown of SFKs in HMVEC-Ls through siRNA.** HMVEC-Ls were transfected with siRNAs targeting the four SFKs expressed in HMVEC-Ls, c-*SRC*, *YES*, *FYN*, and *LYN*, or control siRNAs. *A*, after 72 h, ECs were processed for immunoblotting with antibodies against each of these four SFK proteins. Blots were stripped and reprobed for β-tubulin. These blots are representative of three experiments. *B*, ECs were processed for a cell-based ELISA to detect phospho-Tyr^{416} as a measure of SFK activation. The phospho-Tyr^{416} was normalized to both total SFK and cellular protein and expressed as mean ± S.E. -fold increase relative to the simultaneous medium control. *n*, the numbers of wells studied, was 6 for each group. *C*, HMVEC-Ls were transfected with siRNAs specifically targeting c-*SRC*, *YES*, *FYN*, or control siRNAs. After 72 h, ECs were exposed for 4 h with LPS (100 ng/ml) or medium alone and lysed, and the lysates were immunoprecipitated with anti-VE-cadherin or anti-p120^{ctn} antibodies. The immunoprecipitates were resolved by SDS-PAGE and transferred to PVDF, and the blots were probed with anti-phosphotyrosine antibodies. To normalize phosphotyrosine signal to immunoprecipitated protein, the immunoblots were stripped and reprobed with the immunoprecipitating antibodies raised against VE-cadherin and p120^{ctn}. These blots are representative of four experiments. *D*, on each immunoblot, densitometric quantification of phosphotyrosine signal of VE-cadherin and p120^{ctn} immunoprecipitates each were normalized to total VE-cadherin and p120^{ctn} signal, respectively. *Vertical bars* represent mean ± S.E. -fold increase of arbitrary densitometry units of phosphotyrosine signal normalized to arbitrary densitometry units of total signal relative to the simultaneous control. $n = 4$. *E*, for the barrier assay, HMVEC-Ls cultured to 70% confluence in plastic dishes were transfected with siRNA targeting *FYN*, c-*SRC*, *LYN*, *YES*, or control siRNAs. After 24 h, transfected cells were seeded onto the filters in assay chambers and cultured for 48 h, after which base line barrier function was established. Only EC monolayers that retained ≥97% of the tracer molecule were exposed for 6 h to 100 ng/ml LPS or medium alone and again assayed for transendothelial [^{14}C]BSA flux. *Vertical bars* represent mean ± S.E. transendothelial [^{14}C]BSA flux in pmol/h immediately after the 6-h study period. *n* indicates the number of monolayers studied and is indicated *within* each *bar*. In *A* and *C*, *IP*, immunoprecipitate; *IB*, immunoblot; *IB**, immunoblot after stripping. In *B*, *D*, and *E*, *, significantly increased compared with the simultaneous medium with control siRNA at $p < 0.05$; **, significantly decreased compared with LPS and control siRNA at $p < 0.05$. In *B* and *E*, the data sets were generated from three independent experiments with 2–4 replicates/treatment/experiment. In *C*, the data were generated from four independent experiments, and the mean ± S.E. changes of the combined data are displayed in *D*.

TLR4-mediated SFK activation. LPS activates FYN, c-SRC, and YES, and these three SFKs play redundant but not totally compensatory roles in LPS-induced barrier dysfunction. They also perform differential functions in regulating ZA protein tyrosine phosphorylation. For VE-cadherin phosphorylation, other SFKs could not compensate for either c-SRC or FYN, whereas they partially offset the effect of YES depletion. These results are compatible with unique roles for c-SRC and FYN. In contrast, for p120^{ctn} phosphorylation, other SFKs could only provide partial compensation for the effect of selective depletion of each of these three SFKs. It is still unknown which other elements in the TLR4 signaling pathway, such as MyD88 and TRAF6, are involved. How FYN, c-SRC, and YES regulate phosphorylation of distinct tyrosine residues within each ZA protein is also under investigation. Since SFK-selective inhibitors only partially protected against LPS-induced barrier disruption, determination of whether other PTK(s) participate in the barrier response to LPS requires further study.

REFERENCES

1. Martin, G. S., Mannino, D. M., Eaton, S., and Moss, M. (2003) *N. Engl. J. Med.* **348,** 1546–1554
2. Bone, R. C. (1993) *Clin. Microbiol. Rev.* **6,** 57–68
3. Ulevitch, R. J., Cochrane, C. G., Henson, P. M., Morrison, D. C., and Doe, W. F. (1975) *J. Exp. Med.* **142,** 1570–1590
4. Brigham, K. L., and Meyrick, B. (1986) *Am. Rev. Respir. Dis.* **133,** 913–927
5. Brandtzaeg, P., Kierulf, P., Gaustad, P., Skulberg, A., Bruun, J. N., Halvorsen, S., and Sorensen, E. (1989) *J. Infect. Dis.* **159,** 195–204
6. Bannerman, D. D., Fitzpatrick, M. J., Anderson, D. Y., Bhattacharjee, A. K., Novitsky, T. J., Hasday, J. D., Cross, A. S., and Goldblum, S. E. (1998) *Infect. Immun.* **66,** 1400–1407
7. Cross, A. (1996) *Shock* **6,** Suppl. 1, 71–74
8. Dauphinee, S. M., and Karsan, A. (2006) *Lab. Invest.* **86,** 9–22
9. Volk, T., and Kox, W. J. (2000) *Inflamm. Res.* **49,** 185–198
10. Angelini, D. J., Hyun, S. W., Grigoryev, D. N., Garg, P., Gong, P., Singh, I. S., Passaniti, A., Hasday, J. D., and Goldblum, S. E. (2006) *Am. J. Physiol.* **291,** L1232–L1245
11. Bannerman, D. D., and Goldblum, S. E. (1997) *Am. J. Physiol.* **273,** L217–L226
12. Poltorak, A., He, X., Smirnova, I., Liu, M. Y., Van Huffel, C., Du, X., Birdwell, D., Alejos, E., Silva, M., Galanos, C., Freudenberg, M., Ricciardi-Castagnoli, P., Layton, B., and Beutler, B. (1998) *Science* **282,** 2085–2088
13. Hoshino, K., Takeuchi, O., Kawai, T., Sanjo, H., Ogawa, T., Takeda, Y., Takeda, K., and Akira, S. (1999) *J. Immunol.* **162,** 3749–3752
14. Andreakos, E., Sacre, S. M., Smith, C., Lundberg, A., Kiriakidis, S., Stonehouse, T., Monaco, C., Feldmann, M., and Foxwell, B. M. (2004) *Blood* **103,** 2229–2237
15. Dunzendorfer, S., Lee, H. K., Soldau, K., and Tobias, P. S. (2004) *FASEB J.* **18,** 1117–1119
16. Zhang, F. X., Kirschning, C. J., Mancinelli, R., Xu, X. P., Jin, Y., Faure, E., Mantovani, A., Rothe, M., Muzio, M., and Arditi, M. (1999) *J. Biol. Chem.* **274,** 7611–7614
17. Faure, E., Equils, O., Sieling, P. A., Thomas, L., Zhang, F. X., Kirschning, C. J., Polentarutti, N., Muzio, M., and Arditi, M. (2000) *J. Biol. Chem.* **275,** 11058–11063
18. Spitzer, J. H., Visintin, A., Mazzoni, A., Kennedy, M. N., and Segal, D. M. (2002) *Eur. J. Immunol.* **32,** 1182–1187
19. Dunzendorfer, S., Lee, H. K., Soldau, K., and Tobias, P. S. (2004) *J. Immunol.* **173,** 1166–1170
20. Guillot, L., Medjane, S., Le-Barillec, K., Balloy, V., Danel, C., Chignard, M., and Si-Tahar, M. (2004) *J. Biol. Chem.* **279,** 2712–2718
21. Hornef, M. W., Frisan, T., Vandewalle, A., Normark, S., and Richter-Dahlfors, A. (2002) *J. Exp. Med.* **195,** 559–570
22. Frey, E. A., Miller, D. S., Jahr, T. G., Sundan, A., Bazil, V., Espevik, T., Finlay, B. B., and Wright, S. D. (1992) *J. Exp. Med.* **176,** 1665–1671
23. Beekhuizen, H., Blokland, I., Corsel-van Tilburg, A. J., Koning, F., and van Furth, R. (1991) *J. Immunol.* **147,** 3761–3767
24. Jersmann, H. P., Hii, C. S., Hodge, G. L., and Ferrante, A. (2001) *Infect. Immun.* **69,** 479–485
25. von Asmuth, E. J., Dentener, M. A., Bazil, V., Bouma, M. G., Leeuwenberg, J. F., and Buurman, W. A. (1993) *Immunology* **80,** 78–83
26. Goldblum, S. E., Ding, X., Brann, T. W., and Campbell-Washington, J. (1993) *J. Cell. Physiol.* **157,** 13–23
27. Horwood, N. J., Mahon, T., McDaid, J. P., Campbell, J., Mano, H., Brennan, F. M., Webster, D., and Foxwell, B. M. (2003) *J. Exp. Med.* **197,** 1603–1611
28. Jefferies, C. A., Doyle, S., Brunner, C., Dunne, A., Brint, E., Wietek, C., Walch, E., Wirth, T., and O'Neill, L. A. (2003) *J. Biol. Chem.* **278,** 26258–26264
29. Napolitani, G., Bortoletto, N., Racioppi, L., Lanzavecchia, A., and D'Oro, U. (2003) *Eur. J. Immunol.* **33,** 2832–2841
30. Henricson, B. E., Carboni, J. M., Burkhardt, A. L., and Vogel, S. N. (1995) *Mol Med* **1,** 428–435
31. Hazeki, K., Masuda, N., Funami, K., Sukenobu, N., Matsumoto, M., Akira, S., Takeda, K., Seya, T., and Hazeki, O. (2003) *Eur. J. Immunol.* **33,** 740–747
32. Hamajima, Y., Fujieda, S., Sunaga, H., Yamada, T., Moribe, K., Watanabe, N., and Murakami, S. (2007) *Auris Nasus Larynx* **34,** 49–56
33. Zhou, Y. Q., Chen, Y. Q., Fisher, J. H., and Wang, M. H. (2002) *J. Biol. Chem.* **277,** 38104–38110
34. Lidington, D., Tyml, K., and Ouellette, Y. (2002) *J. Cell Physiol.* **193,** 373–379
35. Shen, Y., Sultana, C., Arditi, M., Kim, K. S., and Kalra, V. K. (1998) *Am. J. Physiol.* **275,** E479–E486
36. Andriopoulou, P., Navarro, P., Zanetti, A., Lampugnani, M. G., and Dejana, E. (1999) *Arterioscler. Thromb. Vasc. Biol.* **19,** 2286–2297
37. Goldblum, S. E., Young, B. A., Wang, P., and Murphy-Ullrich, J. E. (1999) *Mol. Biol. Cell* **10,** 1537–1551
38. Young, B. A., Wang, P., and Goldblum, S. E. (1998) *Biochem. Biophys. Res. Commun.* **251,** 320–327
39. Esser, S., Lampugnani, M. G., Corada, M., Dejana, E., and Risau, W. (1998) *J. Cell Sci.* **111,** 1853–1865
40. Dejana, E., Corada, M., and Lampugnani, M. G. (1995) *FASEB J.* **9,** 910–918
41. Lampugnani, M. G., and Dejana, E. (1997) *Curr. Opin. Cell Biol.* **9,** 674–682
42. McIntire, F. C., Sievert, H. W., Barlow, G. H., Finley, R. A., and Lee, A. Y. (1967) *Biochemistry* **6,** 2363–2372
43. Sui, X. F., Kiser, T. D., Hyun, S. W., Angelini, D. J., Del Vecchio, R. L., Young, B. A., Hasday, J. D., Romer, L. H., Passaniti, A., Tonks, N. K., and Goldblum, S. E. (2005) *Am. J. Pathol.* **166,** 1247–1258
44. Bannerman, D. D., and Goldblum, S. E. (1999) *Lab. Invest.* **79,** 1181–1199
45. Dobrovolskaia, M. A., Medvedev, A. E., Thomas, K. E., Cuesta, N., Toshchakov, V., Ren, T., Cody, M. J., Michalek, S. M., Rice, N. R., and Vogel, S. N. (2003) *J. Immunol.* **170,** 508–519
46. Martin, G. S. (2001) *Nat. Rev. Mol. Cell Biol.* **2,** 467–475
47. Boggon, T. J., and Eck, M. J. (2004) *Oncogene* **23,** 7918–7927
48. Bull, H. A., Brickell, P. M., and Dowd, P. M. (1994) *FEBS Lett.* **351,** 41–44
49. Achen, M. G., Clauss, M., Schnurch, H., and Risau, W. (1995) *Differentiation* **59,** 15–24
50. Hanke, J. H., Gardner, J. P., Dow, R. L., Changelian, P. S., Brissette, W. H., Weringer, E. J., Pollok, B. A., and Connelly, P. A. (1996) *J. Biol. Chem.* **271,** 695–701
51. Blake, R. A., Broome, M. A., Liu, X., Wu, J., Gishizky, M., Sun, L., and Courtneidge, S. A. (2000) *Mol. Cell Biol.* **20,** 9018–9027
52. Scheifele, D. W., Olsen, E. M., and Pendray, M. R. (1985) *Am. J. Clin. Pathol.* **83,** 227–229
53. Stief, T. W., Ijagha, O., Weiste, B., Herzum, I., Renz, H., and Max, M. (2007) *Blood Coagul. Fibrinolysis* **18,** 179–186
54. Feingold, K. R., Funk, J. L., Moser, A. H., Shigenaga, J. K., Rapp, J. H., and Grunfeld, C. (1995) *Infect. Immun.* **63,** 2041–2046
55. Gegner, J. A., Ulevitch, R. J., and Tobias, P. S. (1995) *J. Biol. Chem.* **270,** 5320–5325
56. Prins, J. M., van Agtmael, M. A., Kuijper, E. J., van Deventer, S. J., and

Speelman, P. (1995) *J. Infect. Dis.* **172,** 886–891
57. Dofferhoff, A. S., Nijland, J. H., de Vries-Hospers, H. G., Mulder, P. O., Weits, J., and Bom, V. J. (1991) *Scand. J. Infect. Dis.* **23,** 745–754
58. Paludan, S. R. (2000) *J. Leukocyte Biol.* **67,** 18–25
59. Chaouat, G. (1994) *Cell Immunol.* **157,** 328–340
60. Geller, D. A., Nussler, A. K., Di Silvio, M., Lowenstein, C. J., Shapiro, R. A., Wang, S. C., Simmons, R. L., and Billiar, T. R. (1993) *Proc. Natl. Acad. Sci. U. S. A.* **90,** 522–526
61. Wu, N. Z., and Baldwin, A. L. (1992) *Am. J. Physiol.* **262,** H1238–H1247
62. Coughlin, S. R. (2000) *Nature* **407,** 258–264
63. Adamson, R. H., Zeng, M., Adamson, G. N., Lenz, J. F., and Curry, F. E. (2003) *Am. J. Physiol.* **285,** H406–H417
64. Puhlmann, M., Weinreich, D. M., Farma, J. M., Carroll, N. M., Turner, E. M., and Alexander, H. R., Jr. (2005) *J. Transl. Med.* **3,** 37
65. Andonegui, G., Bonder, C. S., Green, F., Mullaly, S. C., Zbytnuik, L., Raharjo, E., and Kubes, P. (2003) *J. Clin. Invest.* **111,** 1011–1020
66. Medvedev, A. E., Piao, W., Shoenfelt, J., Rhee, S. H., Chen, H., Basu, S., Wahl, L. M., Fenton, M. J., and Vogel, S. N. (2007) *J. Biol. Chem.* **282,** 16042–16053
67. Johnsen, I. B., Nguyen, T. T., Ringdal, M., Tryggestad, A. M., Bakke, O., Lien, E., Espevik, T., and Anthonsen, M. W. (2006) *EMBO J.* **25,** 3335–3346
68. Wang, K. Z., Wara-Aswapati, N., Boch, J. A., Yoshida, Y., Hu, C. D., Galson, D. L., and Auron, P. E. (2006) *J. Cell Sci.* **119,** 1579–1591
69. Funakoshi-Tago, M., Tago, K., Sonoda, Y., Tominaga, S., and Kasahara, T. (2003) *Eur. J. Biochem.* **270,** 1257–1268
70. Mukundan, L., Milhorn, D. M., Matta, B., and Suttles, J. (2004) *Cell. Signal.* **16,** 375–384
71. Shao, M. X., Ueki, I. F., and Nadel, J. A. (2003) *Proc. Natl. Acad. Sci. U. S. A.* **100,** 11618–11623
72. Kang, J. L., Lee, H. W., Lee, H. S., Pack, I. S., Chong, Y., Castranova, V., and Koh, Y. (2001) *Am. J. Respir. Crit. Care Med.* **164,** 2206–2212
73. Ruetten, H., and Thiemermann, C. (1997) *Br. J. Pharmacol.* **122,** 59–70
74. Schmitz, G., and Orso, E. (2002) *Curr. Opin. Lipidol.* **13,** 513–521
75. Kang, J. L., Lee, H. W., Kim, H. J., Lee, H. S., Castranova, V., Lim, C. M., and Koh, Y. (2005) *J. Toxicol. Environ. Health A* **68,** 1643–1662
76. Kox, M., Wijetunge, S., Pickkers, P., and Hughes, A. D. (2007) *Vascul. Pharmacol.* **46,** 195–200
77. Paul, R., Zhang, Z. G., Eliceiri, B. P., Jiang, Q., Boccia, A. D., Zhang, R. L., Chopp, M., and Cheresh, D. A. (2001) *Nat. Med.* **7,** 222–227
78. Castano, J., Solanas, G., Casagolda, D., Raurell, I., Villagrasa, P., Bustelo, X. R., Garcia de Herreros, A., and Dunach, M. (2007) *Mol. Cell. Biol.* **27,** 1745–1757
79. Severgnini, M., Takahashi, S., Tu, P., Perides, G., Homer, R. J., Jhung, J. W., Bhavsar, D., Cochran, B. H., and Simon, A. R. (2005) *Am. J. Respir. Crit. Care Med.* **171,** 858–867
80. Eliceiri, B. P., Paul, R., Schwartzberg, P. L., Hood, J. D., Leng, J., and Cheresh, D. A. (1999) *Mol. Cell* **4,** 915–924
81. Piedra, J., Miravet, S., Castano, J., Palmer, H. G., Heisterkamp, N., Garcia de Herreros, A., and Dunach, M. (2003) *Mol. Cell Biol.* **23,** 2287–2297
82. Loo, L. W., Kanemitsu, M. Y., and Lau, A. F. (1999) *Mol. Carcinog.* **25,** 187–195
83. Kanemitsu, M. Y., Loo, L. W., Simon, S., Lau, A. F., and Eckhart, W. (1997) *J. Biol. Chem.* **272,** 22824–22831
84. Lu, T. T., Barreuther, M., Davis, S., and Madri, J. A. (1997) *J. Biol. Chem.* **272,** 14442–14446
85. Wallez, Y., Cand, F., Cruzalegui, F., Wernstedt, C., Souchelnytskyi, S., Vilgrain, I., and Huber, P. (2007) *Oncogene* **26,** 1067–1077
86. Lilien, J., Balsamo, J., Arregui, C., and Xu, G. (2002) *Dev. Dyn.* **224,** 18–29
87. Reynolds, A. B., Daniel, J., McCrea, P. D., Wheelock, M. J., Wu, J., and Zhang, Z. (1994) *Mol. Cell Biol.* **14,** 8333–8342
88. Alema, S., and Salvatore, A. M. (2007) *Biochim. Biophys. Acta.* **1773,** 47–58
89. Anastasiadis, P. Z., and Reynolds, A. B. (2000) *J. Cell Sci.* **113,** 1319–1334
90. Lampugnani, M. G., Corada, M., Andriopoulou, P., Esser, S., Risau, W., and Dejana, E. (1997) *J. Cell Sci.* **110,** 2065–2077
91. Lowell, C. A., and Soriano, P. (1996) *Genes Dev.* **10,** 1845–1857